Signal Transduction and Smooth Muscle

Edited by Mohamed Trebak Scott Earley

ISBN: 978–1–4987–7422–2 (hbk)
ISBN: 978–1–315–15458–9 (ebk)

First published 2019

Chapter 9

Mitochondria Structure and Position in the Local Control of Calcium Signals in Smooth Muscle Cells

John G. McCarron, Christopher Saunter, Calum Wilson, John M. Girkin, and Susan Chalmers

CRC Press
Taylor & Francis Group
Boca Raton London New York

CRC Press is an imprint of the
Taylor & Francis Group, an **informa** business

9 Mitochondria Structure and Position in the Local Control of Calcium Signals in Smooth Muscle Cells

John G. McCarron, Christopher Saunter, Calum Wilson, John M. Girkin, and Susan Chalmers

CONTENTS

9.1 INTRODUCTION

Features of Ca^{2+} signals including the amplitude, duration, frequency and location are encoded by various physiological stimuli. These features of the signals are decoded by cells to selectively activate smooth muscle functions that include contraction and proliferation [1–3]. Central, therefore, to an appreciation of how smooth muscle is controlled is an understanding of the regulation of Ca^{2+}. In smooth muscle, Ca^{2+} signals arise from two major sources. The first is the extracellular space from which Ca^{2+} enters the cell via channels such as voltage-dependent Ca^{2+} channels, store-operated Ca^{2+} (SOC) channels and various members of the transient receptor potential channel family. The second major Ca^{2+} source is the internal Ca^{2+} store (sarcoplasmic reticulum; SR) [4–6]. The SR accumulates Ca^{2+} using sarco/endoplasmic reticulum Ca^{2+}-ATPases (SERCA) and Ca^{2+} is released from the SR via the ligand-gated channel/receptor complexes, the IP_3 receptor (IP_3R) and ryanodine receptor (RyR). Release of Ca^{2+} via IP_3R is activated by

IP_3 generated in response to many G-protein or tyrosine kinase-linked receptor activators including drugs [7,8]. RyR may be activated pharmacologically (e.g., caffeine), by Ca^{2+} influx from outside the cell in the process of Ca^{2+}-induced Ca^{2+} release (CICR), or when the stores Ca^{2+} content exceeds normal physiological values, that is in store overload [2,9–12].

Activation of either Ca^{2+} influx or Ca^{2+} release results in an increase of the cytoplasmic Ca^{2+} concentration ($[Ca^{2+}]_c$) from the resting value of ~100 nM to ~1 μM for many seconds throughout the cell, and transiently (e.g., 100 ms) to much higher values (e.g., 50 μM) in small parts of the cytoplasm close to sites of influx or Ca^{2+} release. These local Ca^{2+} signals begin with the opening of one or a few channels, allowing a large flux of the ion into the cytoplasm. Influx to the cytoplasm via voltage-dependent Ca^{2+} channels occurs at rates of ~0.6 million Ca^{2+} ions per second per channel (0.2 pA current). The influx generates a significant local concentration gradient near the channel in which $[Ca^{2+}]$ declines from ~10 μM to ~100 nM over a few hundred nanometers from the plasma membrane [2,13–17]. Voltage-dependent Ca^{2+} channel open time is brief (~1 ms) and the gradient dissipates rapidly with rates of change in the subplasma membrane space on the order of ~5000 μM s^{-1} [2] as compared to a much slower rate of ~0.5 μM s^{-1} in the bulk cytoplasm [2] after a global $[Ca^{2+}]$ rise [18,19]. The large difference in rate of decline in the subplasma membrane space and bulk cytoplasm arise because local changes are driven mostly by buffering and diffusion while the slower rate of decline in bulk cytoplasm is determined by pumps. High local $[Ca^{2+}]$ and the rapid rates of change near channels may target processes with rapid Ca^{2+} binding kinetics to selectively activate particular functions [20–23]. The high local $[Ca^{2+}]$ signals arising from influx also, in turn, may activate IP_3R or RyR to amplify the local signals or propagate through the cell as global signals with slower but more widespread effects [24–30]. The transition of signals from those involving single to multiple channels and from local to global Ca^{2+} increases creates a multitude of signals with various locations, magnitudes and time courses [31–34] so that various cellular biological responses may be selectively activated.

It is acknowledged that a major way that Ca^{2+} signaling specifically targets particular biological processes is by increases in concentration of the ion being selectively localized to certain regions of the cell (Figure 9.1) [36,37]. In native smooth muscle cells, mitochondria contribute to the localization of Ca^{2+} signals and to the modulation of the amplitude of Ca^{2+} signals [38–42]. Mitochondria regulate these local signals by the organelles' ability to take up and release the ion. Ca^{2+} uptake occurs through the mitochondrial Ca^{2+} uniporter while efflux is mediated by the mitochondrial Na^+/Ca^{2+} exchanger. Mitochondrial Ca^{2+} uptake and efflux may regulate cytoplasmic Ca^{2+} concentrations both directly and indirectly. Direct regulation occurs by alteration of bulk Ca^{2+} levels (Figures 9.2 and 9.3) [18,40,44–47]. Indirect regulation occurs as a result of mitochondrial influence on the activity of SR or plasma membrane Ca^{2+} channels. This chapter describes how the structure and positioning of mitochondria contribute to the control of Ca^{2+} signaling, including a previously unrecognized ability of the position of the organelles to increase local Ca^{2+} entry via voltage-dependent Ca^{2+} channels.

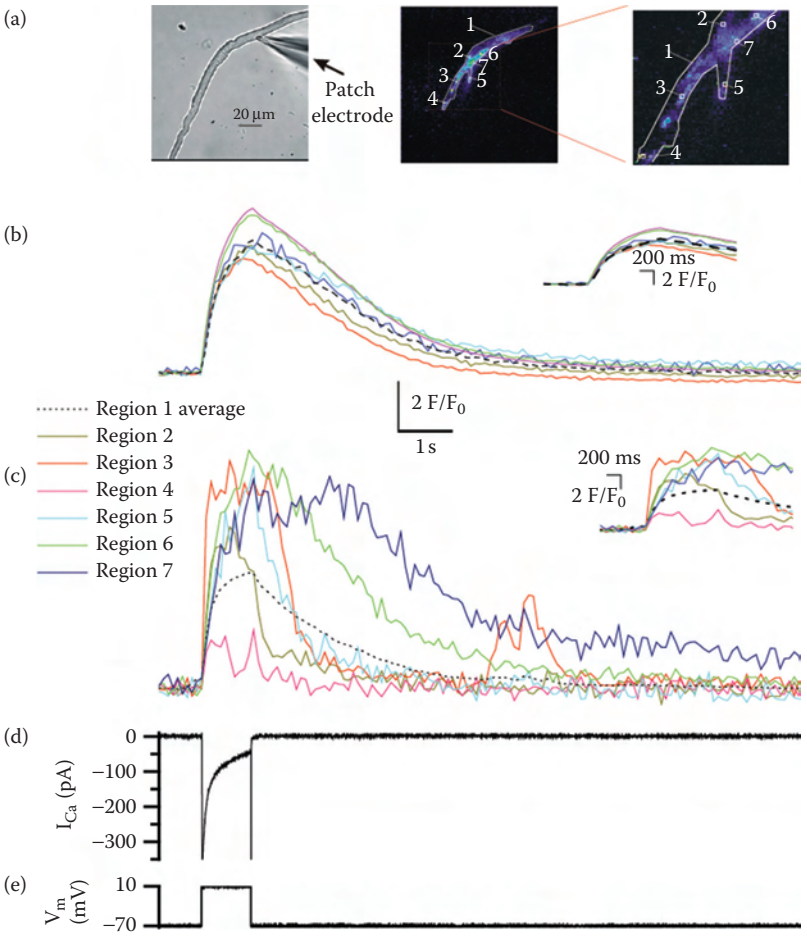

FIGURE 9.1 Simultaneous wide-field epi-fluorescence and total internal reflection fluorescence (TIRF) [Ca^{2+}] measurements in a voltage-clamped smooth muscle. Depolarization (−70 to +10 mV; e), activated a voltage-dependent Ca^{2+} current (I_{Ca}; d) to evoke a rise in [Ca^{2+}] in both the subplasma membrane space (c) and bulk cytoplasm (b). The rise in [Ca^{2+}] that occurred in the subplasma membrane space (measured by TIRF) (c) was more rapid in onset than that seen in the bulk cytoplasm (measured by wide-field epi-fluorescence) (b). Changes in the fluorescence ratio with time (b and c) are each derived from precisely the same 2 × 2-pixel boxes (regions 1–6 in (a), middle and right (expanded) panel; drawn at a 3 × 3-pixel size to facilitate visualization) and from a larger region encompassing the entire TIRF region (region 7). Significantly, while the cytosolic [Ca^{2+}] increase that occurred in the bulk cytoplasm (b) was approximately uniform and simultaneous throughout the cell, those in subplasma membrane space (c) had a wide range of amplitudes and various time courses. Insets in (b) and (c) show the rising phase of the transients on an expanded time base. Black dotted lines are the average responses. (Reproduced from McCarron, J.G. et al., *J. Gen. Physiol*., 133, 439–457, 2009. With permission.)

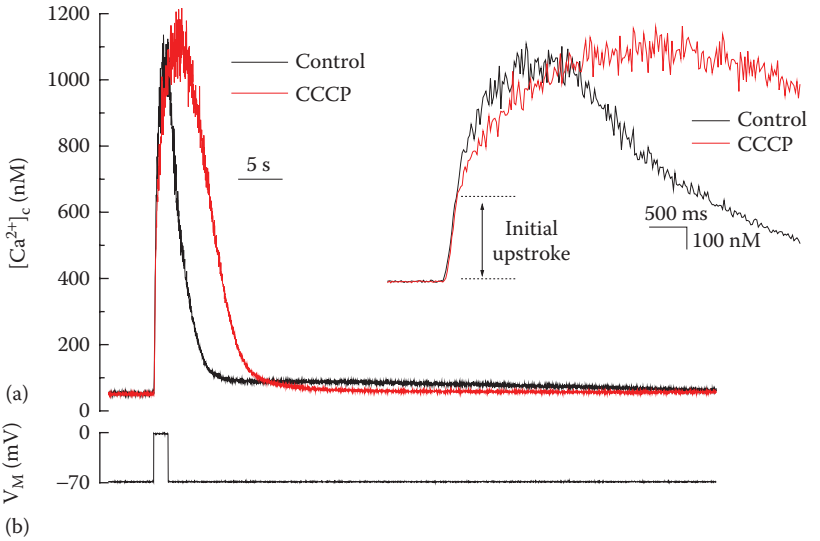

FIGURE 9.2 Preventing mitochondrial Ca^{2+} uptake does not alter the initial upstroke or peak cytosolic [Ca^{2+}] after depolarization-evoked Ca^{2+} entry. Depolarization (–70 to 0 mV; b) of a voltage-clamped single smooth muscle cell activated a voltage-dependent Ca^{2+} current (not shown) and an increased cytosolic [Ca^{2+}] (a). After carbonyl cyanide *m*-chlorophenyl hydrazone (CCCP; 5 μM; transients in red lines) neither the initial rate of cytosolic [Ca^{2+}] rise (see inset) or peak cytosolic [Ca^{2+}] achieved were significantly altered. The insets show the transients on an expanded time base. Cytosolic [Ca^{2+}] was measured at a frequency of 50 Hz using the membrane-impermeable fura-2 (potassium salt, 50 μM) introduced into the cell from the patch pipette. (Reproduced from McCarron, J.G. et al., *Pflugers Arch*., 464, 51–62, 2012. With permission.)

9.2 ROLE OF MITOCHONDRIA IN Ca^{2+} SIGNALING

Mitochondria are major hubs for cellular signaling. In smooth muscle, mitochondria control contractility, proliferation, and growth through regulation of cytoplasmic Ca^{2+} concentrations. A critical feature of mitochondria's ability to control Ca^{2+} signaling is the position and structure of the organelles within cells. Understanding of the precise relationship between Ca^{2+} signaling and mitochondrial structure and position in living, fully-differentiated, (native) cells is preliminary, which may be due to the uncertainty in mitochondrial structure in these cells. Most studies describing mitochondrial structure are derived from cells maintained in culture conditions. Yet, the structure and arrangement of mitochondria in cultured cells differ substantially from the organelles in fully differentiated smooth muscle cells [48–51]. In cultured cells the position of mitochondria contributes significantly to regulation of cytoplasmic Ca^{2+} signals and to the control of mitochondrial Ca^{2+} concentration ($[Ca^{2+}]_m$). For example, SOC increased the $[Ca^{2+}]_m$ in the cultured endothelial cell culture line ECV304, suggesting the organelles accumulate this Ca^{2+} influx. In ECV304 cells, 14% of mitochondria are positioned close to the plasma membrane, a position that will facilitate Ca^{2+} uptake. Less than 4% of mitochondria are close to the internal

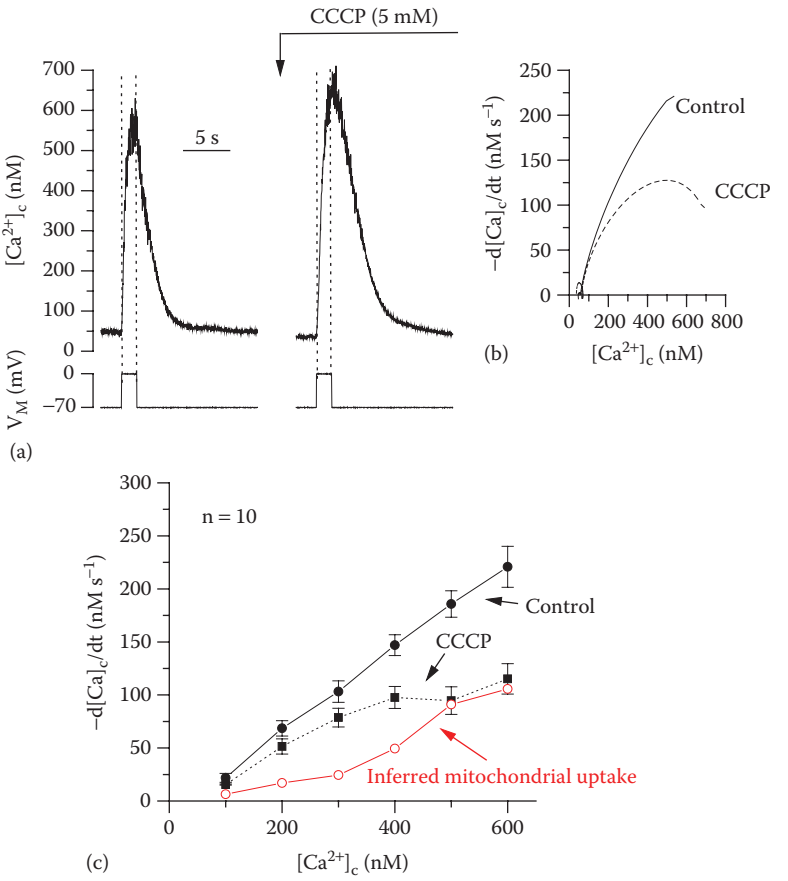

FIGURE 9.3 Mitochondria contribute to cytosolic $[Ca^{2+}]$ decline following voltage-dependent Ca^{2+} entry in smooth muscle. (a) Depolarization (−70 to 0 mV) activated a voltage-dependent Ca^{2+} current (not shown) and increased cytosolic $[Ca^{2+}]$. Carbonyl cyanide *m*-chlorophenyl hydrazone (CCCP; 5 μM) slowed the rate of decline of cytosolic $[Ca^{2+}]$ on repolarization compared with control. (b) The rate of decline of the two transients (a) is shown in (b). The derivative (b) was obtained from high-order polynomial fits to the declining phase of the transient and shows a significant slowing when mitochondria were prevented from accumulating Ca^{2+}. (c) A summary of the rates of decline for ten cells in the presence and absence of CCCP. The inferred mitochondrial contribution to the decline of cytosolic $[Ca^{2+}]$ (red line) was obtained by subtracting control rates from those seen in CCCP and shows that mitochondrial Ca^{2+} uptake occurred above 200 nM $[Ca^{2+}]_c$. (Reproduced from McCarron, J.G. et al., *J. Physiol.*, 516: 149–161, 1999. With permission.)

store and store release of Ca^{2+} did not increase $[Ca^{2+}]_m$. Conversely in HeLa cells, where 65% of mitochondria are close to the internal store and <6% are in close proximity to the plasma membrane, store release of Ca^{2+} caused a much greater increase in $[Ca^{2+}]_m$ than did SOC [52]. These observations suggest mitochondrial position is critical in determining the organelles' uptake of Ca^{2+}. In turn, the position of the mitochondria regulates SOC [53,54]. Forced relocation of mitochondria away from

the cell periphery and towards the nucleus (by overexpressing dynamitin, a protein involved in mitochondrial movement) decreased SOC following store depletion in HeLa cells [55]. These results point to the position of mitochondria as being critical in regulation of Ca^{2+} signaling.

In native fully-differentiated cell types the distribution of mitochondria may also regulate Ca^{2+} signaling. For example, in fully-differentiated cardiac myocytes or neurons, mitochondria appear to be located particularly close to sites of initiation of Ca^{2+} signals from voltage-dependent Ca^{2+} channels on the plasma membrane [56]. At these sites mitochondria contribute to the clearance of Ca^{2+} from the mouth of the channel, limiting Ca^{2+}-dependent inactivation and thus prolonging channel open time [57,58] and facilitating Ca^{2+} entry. In smooth muscle, however, mitochondrial Ca^{2+} uptake does not appear to alter the kinetics of voltage-dependent Ca^{2+} entry (Figure 9.2). This observation suggests the gating of voltage-dependent Ca^{2+} channels is not altered by mitochondria. Notwithstanding the absence of a direct effect on voltage-dependent Ca^{2+} channels, mitochondria may modulate Ca^{2+} rises arising from voltage-dependent Ca^{2+} entry in smooth muscle by modulating Ca^{2+}-dependent feedback processes operative on other ion channels. Mitochondria appear to increase clearance of bulk cytoplasmic Ca^{2+} concentrations, and as a result decrease the activity of Ca^{2+}-activated chloride channels (Cl_{Ca}) [59] and increase the activity of Ca^{2+}-activated K^+ channels (K_{Ca}) [60]. Pharmacological inhibition of the ability of mitochondria to remove Ca^{2+} from the cytoplasm prolonged the activity of Cl_{Ca} in portal vein smooth muscle cells [59] and inhibited K_{Ca} currents in cerebral artery smooth muscle [60]. Modulation of Cl_{Ca} or K_{Ca} will alter the membrane potential to then regulate Ca^{2+} influx via voltage-dependent Ca^{2+} channels as a result.

By taking up Ca^{2+}, mitochondria modulate the time course and amplitude of Ca^{2+} signals to shape the resulting message [1]. For example, we have shown that the Ca^{2+} transient arising from activation of voltage-dependent Ca^{2+} channels has an accelerated rate of decline as a consequence of mitochondrial Ca^{2+} uptake; when uptake is inhibited, the rate of Ca^{2+} decline is substantially slowed (Figures 9.2 and 9.3). In the example shown in Figure 9.3, mitochondria modulate Ca^{2+} signals over the cytosolic [Ca^{2+}] range 600 nM–200 nM, which demonstrates that mitochondria have a high affinity for Ca^{2+} (in the sub-micromolar range; Figure 9.3). Mitochondrial Ca^{2+} uptake does not alter the rate, or extent, of Ca^{2+} *influx* via voltage-dependent Ca^{2+} channels [1] (the likely reasons for this are discussed later on). Some studies have shown that increased mitochondrial reactive oxygen species (ROS) production can alter voltage-dependent Ca^{2+} influx [61], however, this is likely to be due to ROS-dependent alterations in channel open time or conductance, rather than altered mitochondrial Ca^{2+} uptake during voltage-dependent Ca^{2+} influx.

Mitochondria also have the capacity to modulate Ca^{2+} signals that are ~2 orders of magnitude larger than the global Ca^{2+} transient arising from voltage-dependent Ca^{2+} channels and in the tens of micromolar range [62]. One notable example in smooth muscle is mitochondrial regulation of IP_3-mediated Ca^{2+} signals that arise from the activity of a single IP_3R cluster (*Ca^{2+} puffs*; Figure 9.4). When mitochondria are prevented from taking up Ca^{2+} (using uncouplers, complex I inhibitors or uniporter inhibitors), the upstroke of Ca^{2+} puffs is inhibited [42] (Figure 9.4). The duration of the upstroke of a puff is determined by the open time of IP_3R in the cluster.

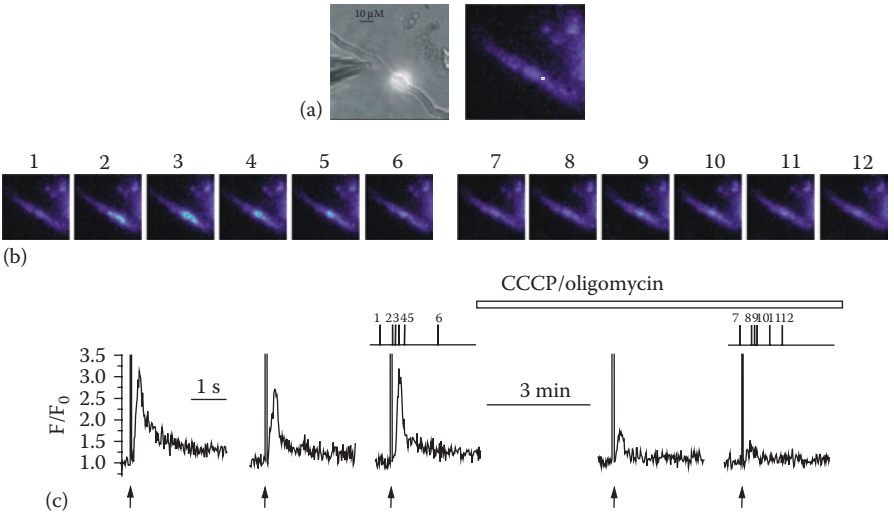

FIGURE 9.4 Preventing mitochondrial Ca^{2+} uptake by depolarizing $\Delta\Psi m$ with CCCP/oligomycin inhibits Ca^{2+} release from IP_3R clusters (Ca^{2+} puffs). At −70 mV, locally photolyzed caged $InsP_3$ (25 μM) (↑, C) in a ~20 μm diameter region (a; bright spot in left-hand panel, see also whole cell electrode, left side) evoked Ca^{2+} puffs in an EGTA (300 μM) buffered smooth muscle cell (b, c). Note: There are two individual Ca^{2+} puff sites in response to photorelease of $InsP_3$; one site releases Ca^{2+} just before the other site. Flash photolysis of $InsP_3$ every ~60 s generated approximately comparable cytosolic [Ca^{2+}] increases. (c) Superfusion of carbonyl cyanide *m*-chlorophenyl hydrazone (CCCP) and oligomycin (1 μM and 6 μM, respectively) while continuing to photolyze $InsP_3$ at ~60 intervals, decreased the amplitude of $InsP_3$-mediated Ca^{2+} puffs (b, c). The cytosolic [Ca^{2+}] images (b) are derived from the time points indicated by the corresponding numbers in (c). Cytosolic $[Ca^{2+}]_c$ changes in (b) are expressed by color; dark blue low and light blue high cytosolic [Ca^{2+}]. Measurements were made from a single 3 × 3-pixel box (a; right hand panel, white square). The large increase in fluorescence at time 0 is the flash artefact triggering photolysis of caged IP_3. (Reproduced from Olson, M.L. et al., *J. Biol. Chem.*, 285, 2040–2050, 2010. With permission.)

The observation [42] that mitochondria modulates the puff upstroke suggests that the organelle's uptake is fast enough to modulate Ca^{2+} concentration near IP_3R clusters during the channels open time, requiring mitochondria to have a very low affinity for Ca^{2+} (Ca^{2+} puffs >10 μM) and to be positioned close to the channel.

Electron microscopy studies of porcine tracheal smooth muscle cells suggest that 99% of mitochondria were within 30 nm of SR and 48% of the mitochondrial outer membrane was within 30 nm with the SR [63] with some mitochondria fully ensheathed by SR [63,64]. Given the proximity between sites of Ca^{2+} release and mitochondria, the question arises as to whether or not there is a direct intermolecular link between the two structures. While there are no high-resolution studies of this link in smooth muscle, electron tomographs [65] and transmission electron micrographs [66] in other cells show tethers that connect the endoplasmic reticulum (ER) to the mitochondrial outer membrane that may be significant in Ca^{2+} signaling. Indeed, immunocytochemical studies show that those regions of the ER in close

proximity to mitochondria are also enriched with IP_3R to create *hotspots* for the transfer of Ca^{2+} from the ER to mitochondria [62]. Several molecular candidates for the tethers have been identified in cell types other than smooth muscle cells. The IP_3R itself has been shown to be tethered to the mitochondrial voltage-dependent anion channel (VDAC) via the chaperone glucose-regulated protein 75 (GRP75), an interaction that promotes mitochondrial accumulation of Ca^{2+} released by IP_3R [67]. Interestingly, both *in vitro* treatment of epithelial cells with high glucose and long-term hyperglycemia in a mouse model of diabetes reduced GRP75 levels, reducing ER-mitochondrial contact sites [68]. The protein mitofusin-2 is located on both mitochondrial and ER membranes and is proposed to form homodimeric tethers between the organelles [69] that contribute to Ca^{2+} signaling. Disrupting linkages between the SR and mitochondria by gene silencing of mitofusin-2 decreased mitochondrial Ca^{2+} uptake during IP_3-mediated $[Ca^{2+}]_c$ rises [65,69]. The multifunctional sorting protein PACS-2, which is localized to the ER and may play a role in apoptotic pathway initiation, has also been proposed to be important for maintaining close apposition of ER and mitochondria in the A7 astrocyte cell line [70]. siRNA silencing of PACS-2 caused mitochondrial fragmentation and separation from the ER, altering Ca^{2+} signaling by increasing IP_3-mediated Ca^{2+} release [70]. The sigma-1 receptor, a protein involved in cell stress responses and present on the ER at regions in close contact with mitochondria, may also couple the membranes of the two organelles [71]. The sigma-1 receptor may form a complex with another chaperone protein (BiP) to stabilize IP_3R at regions of ER-mitochondrial proximity. Depletion of ER Ca^{2+} dissociates the sigma-1 receptor from BiP, leading to prolonged Ca^{2+} signaling into mitochondria via IP_3Rs [71].

The question arises: how can mitochondria—by removing Ca^{2+} from the cytoplasm (i.e., lowering $[Ca^{2+}]$)—generate a larger cytoplasmic $[Ca^{2+}]$ rise? IP_3R are regulated by Ca^{2+}-dependent positive and negative feedback mechanisms [72,73]. By removing Ca^{2+}, mitochondria may limit a negative feedback inhibition of Ca^{2+} on IP_3R [42]. There are at least two types of Ca^{2+}-dependent negative feedback mechanisms that may deactivate smooth muscle IP_3R. In the first, a Ca^{2+}-dependent deactivation of IP_3R occurs at cytosolic $[Ca^{2+}]$ exceeding ~300 nM [73]. The onset is rapid and the deactivation is persistent and lasts for ~5 s after the cytosolic $[Ca^{2+}]$ increase has ended [74]. Another form of Ca^{2+}-dependent deactivation of IP_3R, once initiated by an increased cytosolic $[Ca^{2+}]$, persisted for tens of seconds after cytosolic $[Ca^{2+}]$ had regained resting values, that is, IP_3R became, at least partially, refractory [30,75]. Each of these processes would persistently restrict Ca^{2+} release via IP_3R. Mitochondrial Ca^{2+} uptake, by buffering the Ca^{2+} rise at IP_3R, presumably prevented a persistent deactivation of IP_3R that would otherwise limit the overall release of Ca^{2+} [30,75].

The control that mitochondria exert on Ca^{2+} puffs enables the organelle to exert particularly dramatic effects on the global Ca^{2+} events such as Ca^{2+} waves and oscillations. When mitochondria are prevented from taking up Ca^{2+}, waves and oscillations halt [42,45], that is, modulation of the time course of a Ca^{2+} rise by the organelle determines whether or not some Ca^{2+} signals occur at all. The position and structure of the organelles, together with nano-architectural features of SR-mitochondria junctions, is critical in determining precisely how mitochondria regulate local and global Ca^{2+} signals.

9.3 MITOCHONDRIA STRUCTURE IN NATIVE CELLS

The precise structure and position of mitochondria have been studied most extensively in cultured smooth muscle cells because of the relative ease that the organelles can be visualized in these cells. The thin axial depth of cultured cells and ability to transfect the cells to express unique, mitochondrially-targeted fluorophores result in exceptional signal to noise for imaging mitochondrial structure. In cultured cells, mitochondria exist in a wide range of sizes and shapes (Figure 9.5) and the organelle may change rapidly from solitary ovoid shapes to extensive branched networks and

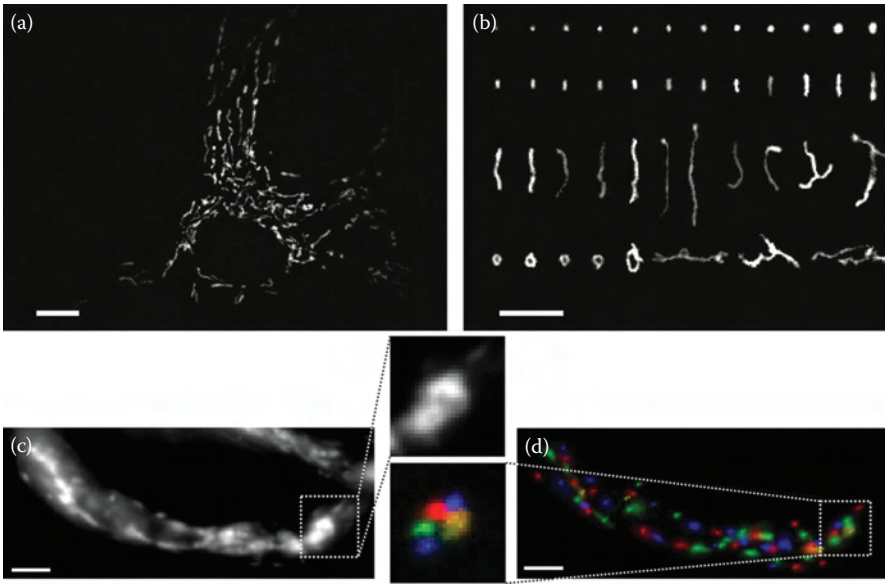

FIGURE 9.5 Mitochondrial structures in cultured and fully-differentiated smooth muscle cells. (a) A cultured single vascular smooth muscle cell showing the arrangement of mitochondria. The organelle is scattered through the cytoplasm and is arranged in various orientations. Mitochondria were labeled with the mitotracker green. (b) Example mitochondria showing the diverse phenotypes which include small spheres, swollen spheres, straight rods, twisted rods, branched rods, and loops. (a and b reproduced from McCarron, J. et al., *J. Vasc. Res.*, 5, 357–371, 2013. With permission.) (c) A native fully-differentiated smooth muscle cell from a cerebral resistance artery showing the arrangement of mitochondria as revealed by the fluorophore tetramethylrhodamine, ethyl ester (TMRE). The organelle is distributed throughout the cytoplasm and appears to be mainly organized parallel to the long axis of the cell. However, the significant axial depth of the cells (when compared to cultured smooth muscle) and multiple overlapping fluorescence point sources result in an optically-confused image with structures that are hard to interpret (d) FaLM permits the size, shape, and position of mitochondria to determined and shows the organelles comprise mainly spheres and short rods. The inset between c and d shows the same example region of the cell before and after application of FaLM. (c and d modified from Chalmers, S. et al., *Nat. Sci. Rep.*, 30, 2000–2013, 2015. With permission.) Scale bars = 10 μm.

even single continuous mitochondrial structure throughout the cell [62,76,77]. This almost continuous re-shaping creates a diversity of structures (Figure 9.5), presumably each with different physiological roles although the precise functions are not yet fully understood [51,78]. On the other hand, mitochondria within fully-differentiated live smooth muscle cells are difficult to visualize because of the significant axial cell depth. This depth results in multiple confused overlapping fluorescence point sources at different distances through the cell derived from various mitochondria. The overlapping fluorescence is difficult to interpret and may be single large organelles or multiple small mitochondria. Exclusive fluorophore targeting is also more difficult in native cells than in cultured cells. Whether or not the arrangements of mitochondria seen in cultured cells occur in fully-differentiated cells is uncertain.

Live cell imaging is required to appreciate the precise relationship between position and structure of mitochondria and the control of Ca^{2+} signaling in fully-differentiated cells. Confocal or other optical sectioning imaging methods do not provide sufficient resolution to determine detailed structure of the organelle in fully-differentiated cells. Detailed insights into the structure of individual mitochondria at fixed points in time have been provided by electron microscopy [EM; 79]. However, EM cannot easily resolve the entire cellular mitochondrial complement or provide information on dynamic changes or functional connectivity and is not compatible with Ca^{2+} imaging. EM [80] and super-resolution techniques [81–89] do not unambiguously reveal the extent of the electrically-continuous inner mitochondrial membrane and are less suited to simultaneously studying Ca^{2+} signaling in live cells, nor do they currently have the imaging speed frequently required.

We recently developed a technique to determine the structure of individual, electrically-discrete mitochondria in live, fully-differentiated cells using conventional fluorescence imaging. Our approach is rapid and quantifies the shape, size and location of mitochondria even when the organelles are densely clustered. The approach measures transient changes in the membrane potential that are unique to each mitochondrion to determine their individual shapes. Changes in membrane potential ($\Delta\Psi m$) arise from transient openings of the mitochondrial permeability transition pore [mPTP; 90,91] and can be visualized using a rapidly-repartitioning cationic fluorophore such as TMRE, as *flickers* of fluorescence [92,93]. These flickers demarcate individual, electrically-discrete mitochondria [92,94]. Drawing inspiration from PALM/BaLM super-resolution techniques [81,82], we used these flicker events to extract structural information of each organelle, facilitating a more detailed analysis of the live-cell fluorescence images. These mitochondrial flickers differ from the correlation of photo-activation, bleaching, or blinking in PALM/BaLM because the flickering objects are not single molecule emitters with a well-defined point-spread function but extended organelles of unknown shape. Nonetheless, the size, shape, and position of the mitochondria can be rapidly determined to the conventional resolution limit from a pixel-by-pixel spatio-temporal covariance of the derived flickering fluorescence signals in an approach that we call Flicker-assisted Localization Microscopy (FaLM) [49,50].

Using FaLM, we found that mitochondria in fully-differentiated resistance artery smooth muscle cells were distributed through the cytoplasm as solitary, spherical-, or short rod-shaped entities (Figure 9.5) [50]. We found mitochondria had a median

area of 0.46 μm^2, a median length of 0.9 μm, and a median length:width ratio of 1.5. We also found the median density of mitochondria in resistance artery smooth muscle cells was 0.125 mitochondria per μm^2 and that mitochondria occupied 7.0% of the cell volume. Each mitochondrion had 2–5 immediate neighbors with ~2 μm between the organelle centers. The mean center distance of a mitochondria from the plasma membrane was ~2 μm [49]. Given a width of mitochondria of 0.6 μm, then, the edge distance of the organelle from the plasma membrane is 1.4 μm. The opening of a single voltage-dependent Ca^{2+} channel (0.2 pA current, mean open-time 1 ms) generates a high local [Ca^{2+}] that decreases steeply with distance from the plasma membrane as the ion diffuses into an increasing hemispheric volume. At a distance of 1.4 μm from the plasma membrane the [Ca^{2+}] arising from the opening of the channel is only ~5 nM above resting values (assuming a buffer power of 100). It is unlikely that this microdomain of Ca^{2+} will be significantly altered by mitochondria. Clearly, the local rise in [Ca^{2+}], and potential contribution of mitochondria, will increase if more than one channel opens or if mitochondria position is different as occurs in some other cell types.

9.4 MITOCHONDRIAL POSITION AND SIGNALING VIA VOLTAGE-DEPENDENT Ca^{2+} CHANNELS

Mitochondria situated immediately at sites of Ca^{2+} influx or release into the cytoplasm may form part of subcellular Ca^{2+}-signaling microdomains and have a privileged access to Ca^{2+} from these sites [38,42,44,62,95]. While, in smooth muscle, Ca^{2+} influx via voltage-dependent Ca^{2+} channels appears not to be tightly controlled at a local level by mitochondria (Figure 9.2) [44,45], nonetheless, the sites of mitochondria near the plasma membrane are associated with *larger* Ca^{2+} signals than elsewhere in the plasma membrane (Figure 9.6). Thus, a single voltage-clamped cerebral resistance artery smooth muscle cell, activated with a depolarizing pulse (–70 to 0 mV) responded with voltage-dependent Ca^{2+} entry and a rise in cytoplasmic Ca^{2+} concentration (Figure 9.6). In this same cell, mitochondrial position was determined (Figure 9.6) using the ΔΨm-sensitive dye TMRE (see Section 9.3). Interestingly, the amplitude of the local rise in cytoplasmic Ca^{2+} concentration was largest at these sites close to mitochondria (Figure 9.6).

After the depolarization ended, at precisely the same sites, there was a substantial undershoot in the cytoplasmic Ca^{2+} concentration when compared to regions away from mitochondria (Figure 9.6). These results suggest that mitochondria may regulate (increase) voltage-dependent Ca^{2+} entry and aid the removal of Ca^{2+} from the cytoplasm positioned close to the plasma membrane.

The upstroke of the voltage-dependent Ca^{2+} transient is unaltered when mitochondria are prevented from taking up Ca^{2+} (Figure 9.2), which suggests that mitochondria are not regulating channel gating. The question arises as to how do mitochondria regulate voltage-dependent Ca^{2+} entry? One possibility is that mitochondria are not involved in the short-term regulation of Ca^{2+} entry but rather in the longer-term level of either expression or distribution of the voltage-dependent Ca^{2+} channel. IP_3-mediated Ca^{2+} release has been shown to induce mitochondrial-ROS generation,

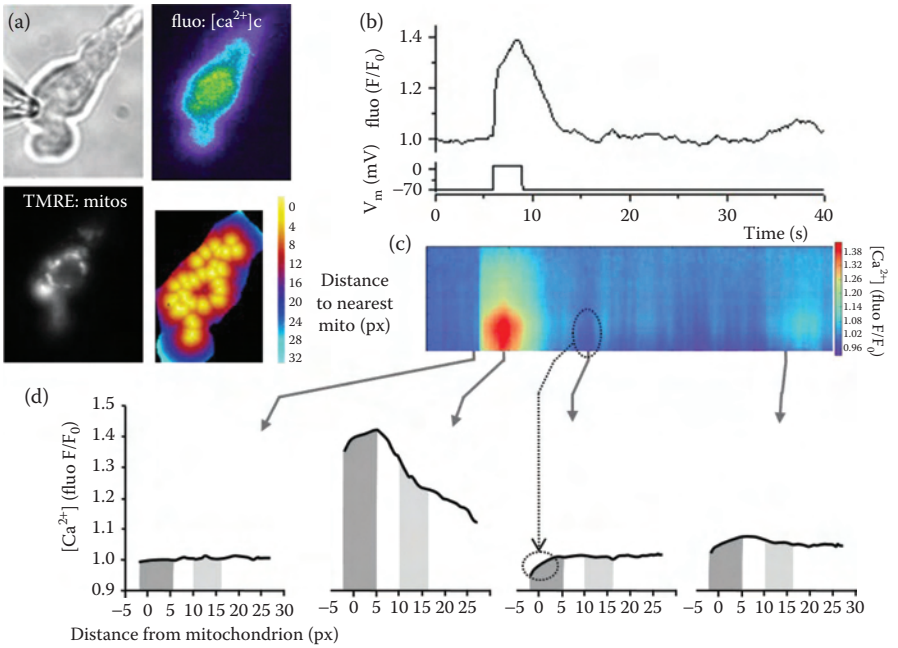

FIGURE 9.6 Mitochondrial position and the magnitude of $[Ca^{2+}]$ changes arising from voltage-dependent Ca^{2+} entry. Depolarization (−70 to 0 mV; b), of a single voltage-clamped smooth muscle cell (a—upper left panel) activated a voltage-dependent Ca^{2+} current (not shown) and rise in $[Ca^{2+}]$ (a—upper right panel, b, and c). The rise in $[Ca^{2+}]$ declined after the depolarization ended. Mitochondrial position was determined at the same time by labeling the organelles with TMRE (a—lower left panel). The magnitude of the rise in $[Ca^{2+}]$ throughout the cell (b and c) was compared on a pixel-by-pixel basis to the center of mass of each nearest mitochondrion (a—lower left and right panels). The rise in $[Ca^{2+}]$ was largest close to a mitochondrion (c and d). In (c) the Ca^{2+} signal in each pixel is plotted as a function of time (x-axis; same scale as b) and distance to the nearest mitochondrion (left y-axis). The magnitude of the $[Ca^{2+}]$ is colored—red high, blue low. After the depolarization had ended, (b) there was an undershoot in $[Ca^{2+}]$ at those regions closest to a mitochondrion (c; shown as darker blue regions and indicated by the dotted lines). (d) Plots the pixel $[Ca^{2+}]$ as a function of distance from the nearest mitochondrion (0 on the x axis is the mitochondrial position) at 4 time points indicated by the arrows from (c). The shaded regions highlight the differences in Ca^{2+} signals close (darker gray) and further (lighter gray) from a mitochondrion. Those regions that are closest to mitochondria experience the highest $[Ca^{2+}]$ concentration after a depolarization and the greatest undershoot (indicated by the dotted lines) as $[Ca^{2+}]$ returns to resting values.

activate the transcription factor NF-kappaB, and stimulate voltage-dependent Ca^{2+} channel transcription [96]. It is tempting to speculate that mitochondria may therefore control voltage-dependent Ca^{2+} channel expression following persistent entry via voltage-dependent Ca^{2+} channels. It is also tempting to speculate that the regional changes in Ca^{2+} (Figure 9.1) arising from voltage-dependent Ca^{2+} channel entry arise from mitochondrial control of the distribution of the channel. The localized decreases in Ca^{2+} near mitochondria also offer support to the proposed control mechanisms operating to regulate and maintain IP_3-mediated Ca^{2+} release (Figure 9.4).

ACKNOWLEDGMENTS

This work was funded by the Wellcome Trust (092292/Z/10/Z; 202924/Z/16/Z) and the British Heart Foundation (PG/16/54/32230; PG16/82/32439), whose support is gratefully acknowledged. CW is supported by a Sir Henry Wellcome Postdoctoral Research Fellowship (204682/Z/16/Z).

REFERENCES

1. Chalmers, S, Olson, ML, MacMillan, D, Rainbow, RD, McCarron, JG. Ion channels in smooth muscle: Regulation by the sarcoplasmic reticulum and mitochondria. *Cell Calcium* 42: 447–466, 2007.
2. McCarron, JG, Chalmers, S, Bradley, KN, Macmillan, D, Muir, TC. Ca^{2+} microdomains in smooth muscle. *Cell Calcium* 40: 461–493, 2006.
3. Sanders, KM. Invited review: Mechanisms of calcium handling in smooth muscles. *J Appl Physiol* 91: 1438–1449, 2001.
4. Macmillan, D, McCarron, JG. The phospholipase C inhibitor U-73122 inhibits Ca(2+) release from the intracellular sarcoplasmic reticulum Ca(2+) store by inhibiting Ca(2+) pumps in smooth muscle. *Br J Pharmacol* 160: 1295–1301, 2010.
5. McCarron, JG, Olson, ML. A single luminally continuous sarcoplasmic reticulum with apparently separate Ca^{2+} stores in smooth muscle. *J Biol Chem* 283: 7206–7218, 2008.
6. Rainbow, RD, Macmillan, D, McCarron, JG. The sarcoplasmic reticulum Ca^{2+} store arrangement in vascular smooth muscle. *Cell Calcium* 46: 313–322, 2009.
7. Berridge, MJ. Inositol trisphosphate and calcium signalling mechanisms. *Biochim Biophys Acta* 1793: 933–940, 2009.
8. Lemmon, MA, Schlessinger, J. Cell signaling by receptor tyrosine kinases. *Cell* 141: 1117–1134, 2010.
9. Burdyga, T, Wray, S. Action potential refractory period in ureter smooth muscle is set by Ca sparks and BK channels. *Nature* 436: 559–562, 2005.
10. McCarron, JG, Craig, JW, Bradley, KN, Muir, TC. Agonist-induced phasic and tonic responses in smooth muscle are mediated by $InsP_3$. *J Cell Sci* 115: 2207–2218, 2002.
11. Nelson, MT, Cheng, H, Rubart, M, Santana, LF, Bonev, AD, Knot, HJ, Lederer, WJ. Relaxation of arterial smooth muscle by calcium sparks. *Science* 270: 633–637, 1995.
12. ZhuGe, R, Tuft, RA, Fogarty, KE, Bellve, K, Fay, FS, Walsh, JV, Jr. The influence of sarcoplasmic reticulum Ca^{2+} concentration on Ca^{2+} sparks and spontaneous transient outward currents in single smooth muscle cells. *J Gen Physiol* 113: 215–228, 1999.
13. Aharon, S, Bercovier, M, Parnas, H. Parallel computation enables precise description of Ca^{2+} distribution in nerve terminals. *Bull Math Biol* 58: 1075–1097, 1996.
14. Llinas, R, Sugimori, M, Silver, RB. Microdomains of high calcium concentration in a presynaptic terminal. *Science* 256: 677–679, 1992.
15. Marsault, R, Murgia, M, Pozzan, T, Rizzuto, R. Domains of high Ca^{2+} beneath the plasma membrane of living A7r5 cells. *Embo J* 16: 1575–1581, 1997.
16. Naraghi, M, Neher, E. Linearized buffered Ca^{2+} diffusion in microdomains and its implications for calculation of $[Ca^{2+}]$ at the mouth of a calcium channel. *J Neurosci* 17: 6961–6973, 1997.
17. Schneggenburger, R, Neher, E. Intracellular calcium dependence of transmitter release rates at a fast central synapse. *Nature* 406: 889–893, 2000.
18. Kamishima, T, McCarron, JG. Ca^{2+} removal mechanisms in rat cerebral resistance size arteries. *Biophys J* 75: 1767–1773, 1998.

19. McGeown, JG, McCarron, JG, Drummond, RM, Fay, FS. Calcium-calmodulin-dependent mechanisms accelerate calcium decay in gastric myocytes from Bufo marinus. *J Physiol* 506 (Pt 1): 95–107, 1998.
20. Bao, R, Lifshitz, LM, Tuft, RA, Bellve, K, Fogarty, KE, ZhuGe, R. A close association of RyRs with highly dense clusters of Ca^{2+}-activated Cl^- channels underlies the activation of STICs by Ca^{2+} sparks in mouse airway smooth muscle. *J Gen Physiol* 132: 145–160, 2008.
21. Kargacin, GJ. Responses of Ca^{2+}-binding proteins to localized, transient changes in intracellular [Ca^{2+}]. *J Theor Biol* 221: 245–258, 2003.
22. Macrez, N, Mironneau, J. Local Ca^{2+} signals in cellular signalling. *Curr Mol Med* 4: 263–275, 2004.
23. Zhuge, R, Bao, R, Fogarty, KE, Lifshitz, LM. Ca^{2+} sparks act as potent regulators of excitation-contraction coupling in airway smooth muscle. *J Biol Chem* 285: 2203–2210, 2009.
24. Bai, Y, Edelmann, M, Sanderson, MJ. The contribution of inositol 1,4,5-trisphosphate and ryanodine receptors to agonist-induced Ca^{2+} signaling of airway smooth muscle cells. *Am J Physiol Lung Cell Mol Physiol* 297: L347–L361, 2009.
25. Balemba, OB, Heppner, TJ, Bonev, AD, Nelson, MT, Mawe, GM. Calcium waves in intact guinea pig gallbladder smooth muscle cells. *Am J Physiol Gastrointest Liver Physiol* 291: G717–G727, 2006.
26. Boittin, FX, Macrez, N, Halet, G, Mironneau, J. Norepinephrine-induced Ca^{2+} waves depend on $InsP_3$ and ryanodine receptor activation in vascular myocytes. *Am J Physiol* 277: C139–C151, 1999.
27. Gordienko, DV, Harhun, MI, Kustov, MV, Pucovsky, V, Bolton, TB. Sub-plasmalemmal $[Ca^{2+}]_i$ upstroke in myocytes of the guinea-pig small intestine evoked by muscarinic stimulation: IP_3R-mediated Ca^{2+} release induced by voltage-gated Ca^{2+} entry. *Cell Calcium* 43: 122–141, 2008.
28. Jaggar, JH, Nelson, MT. Differential regulation of Ca^{2+} sparks and Ca^{2+} waves by UTP in rat cerebral artery smooth muscle cells. *Am J Physiol Cell Physiol* 279: C1528–C1539, 2000.
29. McCarron, JG, Chalmers, S, MacMillan, D, Olson, ML. Agonist-evoked Ca^{2+} wave progression requires Ca^{2+} and IP_3. *J Cell Physiol* 244: 334–344, 2010.
30. McCarron, JG, MacMillan, D, Bradley, KN, Chalmers, S, Muir, TC. Origin and mechanisms of Ca^{2+} waves in smooth muscle as revealed by localized photolysis of caged inositol 1,4,5-trisphosphate. *J Biol Chem* 279: 8417–8427, 2004.
31. Bai, Y, Sanderson, MJ. Airway smooth muscle relaxation results from a reduction in the frequency of Ca^{2+} oscillations induced by a cAMP-mediated inhibition of the IP_3 receptor. *Respir Res* 7: 34, 2006.
32. Berridge, MJ, Lipp, P, Bootman, MD. The versatility and universality of calcium signalling. *Nat Rev Mol Cell Biol* 1: 11–21, 2000.
33. Bootman, MD, Berridge, MJ. The elemental principles of calcium signaling. *Cell* 83: 675–678, 1995.
34. Marchant, JS, Parker, I. Role of elementary Ca^{2+} puffs in generating repetitive Ca^{2+} oscillations. *Embo J* 20: 65–76, 2001.
35. McCarron, JG, Olson, ML, Currie, S, Wright, AJ, Anderson, KI, Girkin, JM. Elevations of intracellular calcium reflect normal voltage-dependent behavior, and not constitutive activity, of voltage-dependent calcium channels in gastrointestinal and vascular smooth muscle. *J Gen Physiol* 133: 439–457, 2009.
36. Parekh, AB. Store-operated Ca^{2+} entry: Dynamic interplay between endoplasmic reticulum, mitochondria and plasma membrane. *J Physiol* 547: 333–348, 2003.
37. Rizzuto, R, Brini, M, Murgia, M, Pozzan, T. Microdomains with high Ca^{2+} close to IP_3-sensitive channels that are sensed by neighboring mitochondria. *Science* 262: 744–747, 1993.

38. Arnaudeau, S, Kelley, WL, Walsh, JV, Jr., Demaurex, N. Mitochondria recycle Ca^{2+} to the endoplasmic reticulum and prevent the depletion of neighboring endoplasmic reticulum regions. *J Biol Chem* 276: 29430–29439, 2001.
39. Drummond, RM, Fay, FS. Mitochondria contribute to Ca^{2+} removal in smooth muscle cells. *Pflugers Arch* 431: 473–482, 1996.
40. Drummond, RM, Mix, TC, Tuft, RA, Walsh, JV, Jr., Fay, FS. Mitochondrial Ca^{2+} homeostasis during Ca^{2+} influx and Ca^{2+} release in gastric myocytes from Bufo marinus. *J Physiol* 522: 375–390, 2000.
41. Drummond, RM, Tuft, RA. Release of Ca^{2+} from the sarcoplasmic reticulum increases mitochondrial [Ca^{2+}] in rat pulmonary artery smooth muscle cells. *J Physiol* 516 (Pt 1): 139–147, 1999.
42. Olson, ML, Chalmers, S, McCarron, JG. Mitochondrial Ca^{2+} uptake increases Ca^{2+} release from inositol 1,4,5-trisphosphate receptor clusters in smooth muscle cells. *J Biol Chem* 285: 2040–2050, 2010.
43. McCarron, JG, Olson, ML, Chalmers, S. Mitochondrial regulation of cytosolic Ca^{2+} signals in smooth muscle. *Pflugers Arch* 464: 51–62, 2012.
44. McCarron, JG, Muir, TC. Mitochondrial regulation of the cytosolic Ca^{2+} concentration and the $InsP_3$-sensitive Ca^{2+} store in guinea-pig colonic smooth muscle. *J Physiol* 516: 149–161, 1999.
45. Chalmers, S, McCarron, JG. The mitochondrial membrane potential and Ca^{2+} oscillations in smooth muscle. *J Cell Sci* 121: 75–85, 2008.
46. Kamishima, T, Davies, NW, Standen, NB. Mechanisms that regulate $[Ca^{2+}]_i$ following depolarization in rat systemic arterial smooth muscle cells. *J Physiol* 522: 285–295, 2000.
47. Kamishima, T, McCarron, JG. Regulation of the cytosolic Ca^{2+} concentration by Ca^{2+} stores in single smooth muscle cells from rat cerebral arteries. *J Physiol* 501: 497–508, 1997.
48. Chalmers, S, Saunter, C, Wilson, C, Coats, P, Girkin, JM, McCarron, JG. Mitochondrial motility and vascular smooth muscle proliferation. *Arterioscler Thromb Vasc Biol* 32: 3000–3011, 2012.
49. Chalmers, S, Saunter, CD, Girkin, JM, McCarron, JG. Age decreases mitochondrial motility and increases mitochondrial size in vascular smooth muscle. *J Physiol* 594: 4283–4295, 2016.
50. Chalmers, S, Saunter, CD, Girkin, JM, McCarron, JG. Flicker-assisted localization microscopy reveals altered mitochondrial architecture in hypertension. *Nat Sci Rep* 30: 2000–2013, 2015.
51. McCarron, J, Wilson, C, Sandison, ME, Olson, ML, Girkin, JM, Saunter, C, Chalmers, S. From structure to function: Mitochondrial morphology, motion and shaping in vascular smooth muscle. *J Vasc Res* 5: 357–371, 2013.
52. Lawrie, AM, Rizzuto, R, Pozzan, T, Simpson, AW. A role for calcium influx in the regulation of mitochondrial calcium in endothelial cells. *J Biol Chem* 271: 10753, 1996.
53. Hoth, M, Button, DC, Lewis, RS. Mitochondrial control of calcium-channel gating: A mechanism for sustained signaling and transcriptional activation in T lymphocytes. *Proc Natl Acad Sci USA* 97: 10607–10612, 2000.
54. Hoth, M, Fanger, CM, Lewis, RS. Mitochondrial regulation of store-operated calcium signaling in T lymphocytes. *J Cell Biol* 137: 633–648, 1997.
55. Varadi, A, Cirulli, V, Rutter, GA. Mitochondrial localization as a determinant of capacitative Ca^{2+} entry in HeLa cells. *Cell Calcium* 36: 499, 2004.
56. Barstow, KL, Locknar, SA, Merriam, LA, Parsons, RL. The modulation of action potential generation by calcium-induced calcium release is enhanced by mitochondrial inhibitors in mudpuppy parasympathetic neurons. *Neuroscience* 124: 327, 2004.
57. Hernandez-Guijo, JM, Maneu-Flores, VE, Ruiz-Nuno, A, Villarroya, M, Garcia, AG, Gandia, L. Calcium-dependent inhibition of L, N, and P/Q Ca^{2+} channels in chromaffin cells: Role of mitochondria. *J Neurosci* 21: 2553, 2001.

58. Sanchez, JA, Garcia, MC, Sharma, VK, Young, KC, Matlib, MA, Sheu, SS. Mitochondria regulate inactivation of L-type Ca^{2+} channels in rat heart. *J Physiol* 536: 387–396, 2001.
59. Greenwood, IA, Helliwell, RM, Large, WA. Modulation of Ca^{2+}-activated Cl^- currents in rabbit portal vein smooth muscle by an inhibitor of mitochondrial Ca^{2+} uptake. *J Physiol* 505: 53–64, 1997.
60. Cheranov, SY, Jaggar, JH. Mitochondrial modulation of Ca^{2+} sparks and transient KCa currents in smooth muscle cells of rat cerebral arteries. *J Physiol* 556: 755–771, 2004.
61. Ochi, R, Dhagia, V, Lakhkar, A, Patel, D, Wolin, MS, Gupte, SA. Rotenone-stimulated superoxide release from mitochondrial complex I acutely augments L-type Ca2+ current in A7r5 aortic smooth muscle cells. *Am J Physiol Heart Circ Physiol* 310: H1118–H1128, 2016.
62. Rizzuto, R, Pinton, P, Carrington, W, Fay, FS, Fogarty, KE, Lifshitz, LM, Tuft, RA, Pozzan, T. Close contacts with the endoplasmic reticulum as determinants of mitochondrial Ca^{2+} responses. *Science* 280: 1763–1766, 1998.
63. Dai, J, Kuo, KH, Leo, JM, van Breemen, C, Lee, CH. Rearrangement of the close contact between the mitochondria and the sarcoplasmic reticulum in airway smooth muscle. *Cell Calcium* 37: 333–340, 2005.
64. Nixon, GF, Mignery, GA, Somlyo, AV. Immunogold localization of inositol 1,4,5-trisphosphate receptors and characterization of ultrastructural features of the sarcoplasmic reticulum in phasic and tonic smooth muscle. *J Muscle Res Cell Motil* 15: 682–700, 1994.
65. Csordas, G, Renken, C, Varnai, P, Walter, L, Weaver, D, Buttle, KF, Balla, T, Mannella, CA, Hajnoczky, G. Structural and functional features and significance of the physical linkage between ER and mitochondria. *J Cell Biol* 174: 915–921, 2006.
66. Boncompagni, S, Rossi, AE, Micaroni, M, Beznoussenko, GV, Polishchuk, RS, Dirksen, RT, Protasi, F. Mitochondria are linked to calcium stores in striated muscle by developmentally regulated tethering structures. *Mol Biol Cell* 20: 1058–1067, 2009.
67. Szabadkai, G, Bianchi, K, Varnai, P, De Stefani, D, Wieckowski, MR, Cavagna, D, Nagy, AI, Balla, T, Rizzuto, R. Chaperone-mediated coupling of endoplasmic reticulum and mitochondrial Ca^{2+} channels. *J Cell Biol* 175: 901–911, 2006.
68. Ma, JH, Shen, S, Wang, JJ, He, Z, Poon, A, Li J, Qu, J, Zhang, SX. Comparative proteomic analysis of the mitochondria-associated ER membrane (MAM) in a long-term type 2 diabetic rodent model. *Sci Rep* 7: 2062, 2017.
69. de Brito, OM, Scorrano, L. Mitofusin 2 tethers endoplasmic reticulum to mitochondria. *Nature* 456: 605–610, 2008.
70. Simmen, T, Aslan, JE, Blagoveshchenskaya, AD, Thomas, L, Wan, L, Xiang, Y, Feliciangeli, SF, Hung, CH, Crump, CM, Thomas, G. PACS-2 controls endoplasmic reticulum-mitochondria communication and Bid-mediated apoptosis. *Embo J* 24: 717–729, 2005.
71. Hayashi, T, Su, TP. Sigma-1 receptor chaperones at the ER-mitochondrion interface regulate Ca^{2+} signaling and cell survival. *Cell* 131: 596–610, 2007.
72. Bezprozvanny, I, Watras, J, Ehrlich, BE. Bell-shaped calcium-response curves of Ins(1,4,5)P3- and calcium-gated channels from endoplasmic reticulum of cerebellum. *Nature* 351: 751–754, 1991.
73. Iino, M. Biphasic Ca^{2+} dependence of inositol 1,4,5-trisphosphate-induced Ca^{2+} release in smooth muscle cells of the guinea pig taenia caeci. *J Gen Physiol* 95: 1103–1122, 1990.
74. Iino, M, Tsukioka, M. Feedback control of inositol trisphosphate signalling by calcium. *Mol Cell Endocrinol* 98: 141–146, 1994.

75. Oancea, E, Meyer, T. Reversible desensitization of inositol trisphosphate-induced calcium release provides a mechanism for repetitive calcium spikes. *J Biol Chem* 271: 17253–17260, 1996.
76. De Giorgi, F, Lartigue, L, Ichas, F. Electrical coupling and plasticity of the mitochondrial network. *Cell Calcium* 28: 365–370, 2000.
77. Guillery, O, Malka, F, Frachon, P, Milea, D, Rojo, M, Lombes, A. Modulation of mitochondrial morphology by bioenergetics defects in primary human fibroblasts. *Neuromuscul Disord* 18: 319–330, 2008.
78. Mitra, K, Wunder, C, Roysam, B, Lin, G, Lippincott-Schwartz, J. A hyperfused mitochondrial state achieved at G1-S regulates cyclin E buildup and entry into S phase. *Proc Natl Acad Sci USA* 106: 11960–11965, 2009.
79. Mannella, CA. Structural diversity of mitochondria: Functional implications. *Ann N Y Acad Sci* 1147: 171–179, 2008.
80. Frey, TG, Mannella, CA. The internal structure of mitochondria. *Trends Biochem Sci* 25: 319–324, 2000.
81. Betzig, E, Patterson, GH, Sougrat, R, Lindwasser, OW, Olenych, S, Bonifacino, JS, Davidson, MW, Lippincott-Schwartz, J, Hess, HF. Imaging intracellular fluorescent proteins at nanometer resolution. *Science* 313: 1642–1645, 2006.
82. Burnette, DT, Sengupta, P, Dai, Y, Lippincott-Schwartz, J, Kachar, B. Bleaching/blinking assisted localization microscopy for superresolution imaging using standard fluorescent molecules. *Proc Natl Acad Sci USA* 108: 21081–21086, 2011.
83. Cox, S, Rosten, E, Monypenny, J, Jovanovic-Talisman, T, Burnette, DT, Lippincott-Schwartz, J, Jones, GE, Heintzmann, R. Bayesian localization microscopy reveals nanoscale podosome dynamics. *Nat Methods* 9: 195–200, 2012.
84. Egner, A, Jakobs, S, Hell, SW. Fast 100-nm resolution three-dimensional microscope reveals structural plasticity of mitochondria in live yeast. *Proc Natl Acad Sci USA* 99: 3370–3375, 2002.
85. Hirvonen, LM, Wicker, K, Mandula, O, Heintzmann, R. Structured illumination microscopy of a living cell. *Eur Biophys J* 38: 807–812, 2009.
86. Huang, B, Jones, SA, Brandenburg, B, Zhuang, X. Whole-cell 3D STORM reveals interactions between cellular structures with nanometer-scale resolution. *Nat Methods* 5: 1047–1052, 2008.
87. Jans, DC, Wurm, CA, Riedel, D, Wenzel, D, Stagge, F, Deckers, M, Rehling, P, Jakobs, S. STED super-resolution microscopy reveals an array of MINOS clusters along human mitochondria. *Proc Natl Acad Sci USA* 110: 8936–8941, 2013.
88. Rosenbloom, AB, Lee, SH, To, M, Lee, A, Shin, JY, Bustamante, C. Optimized two-color super resolution imaging of Drp1 during mitochondrial fission with a slow-switching Dronpa variant. *Proc Natl Acad Sci USA* 111: 13093–13098, 2014.
89. Shao, L, Kner, P, Rego, EH, Gustafsson, MG. Super-resolution 3D microscopy of live whole cells using structured illumination. *Nat Methods* 8: 1044–1046, 2011.
90. Giorgio, V, von Stockum, S, Antoniel, M, Fabbro, A, Fogolari, F, Forte, M, Glick GD et al. Dimers of mitochondrial ATP synthase form the permeability transition pore. *Proc Natl Acad Sci USA* 110: 5887–5892, 2013.
91. Halestrap, AP, Richardson, AP. The mitochondrial permeability transition: A current perspective on its identity and role in ischaemia/reperfusion injury. *J Mol Cell Cardiol* 78: 129–141, 2015.
92. O'Reilly, CM, Fogarty, KE, Drummond, RM, Tuft, RA, Walsh, JV, Jr. Quantitative analysis of spontaneous mitochondrial depolarizations. *Biophys J* 85: 3350–3357, 2003.

93. O'Reilly, CM, Fogarty, KE, Drummond, RM, Tuft, RA, Walsh, JV, Jr. Spontaneous mitochondrial depolarizations are independent of SR Ca^{2+} release. *Am J Physiol Cell Physiol* 286: C1139–C1151, 2004.
94. Duchen, MR, Leyssens, A, Crompton, M. Transient mitochondrial depolarizations reflect focal sarcoplasmic reticular calcium release in single rat cardiomyocytes. *J Cell Biol* 142: 975–988, 1998.
95. Hajnoczky, G, Csordas, G, Madesh, M, Pacher, P. The machinery of local Ca^{2+} signalling between sarco-endoplasmic reticulum and mitochondria. *J Physiol* 529 Pt 1: 69, 2000.
96. Narayanan, D, Xi, Q, Pfeffer, LM, Jaggar, JH. Mitochondria control functional CaV1.2 expression in smooth muscle cells of cerebral arteries. *Circ Res* 107: 631–641, 2010.